Atmos. Chem. Phys. Discuss., 9, 24193–24223, 2009
www.atmos-chem-phys-discuss.net/9/24193/2009/

Atmospheric Chemistry and Physics Discussions

This discussion paper is/has been under review for the journal Atmospheric Chemistry and Physics (ACP). Please refer to the corresponding final paper in ACP if available.

Formaldehyde and its relation to CO, PAN, and SO_2 in the Houston-Galveston airshed

B. Rappenglück[1], P. K. Dasgupta[2], M. Leuchner[1,*], Q. Li[2], and W. Luke[3]

[1]Department of Earth and Atmospheric Sciences, University of Houston, Houston, Texas, USA
[2]Department of Chemistry, The University of Texas at Arlington, Arlington, Texas, USA
[3]NOAA-ARL, Silver Spring, Maryland, USA
[*]now at: Fachgebiet für Ökoklimatologie, Technische Universität München, Freising, Germany

Received: 27 October 2009 – Accepted: 3 November 2009 – Published: 12 November 2009

Correspondence to: B. Rappenglück (brappenglueck@uh.edu)

Published by Copernicus Publications on behalf of the European Geosciences Union.

Abstract

The Houston-Galveston Airshed (HGA) is one of the major metropolitan areas in the US that is classified as a nonattainment area of Federal ozone standards. Formaldehyde (HCHO) is a key species in understanding ozone related air pollution; some of the highest HCHO concentrations in North America have been reported for the HGA. We report on HCHO measurements in the HGA from summer 2006. Among several sites, maximum HCHO mixing ratios were observed in the Houston Ship Channel (HSC), a region with a very high density of industrial/petrochemical operations.

HCHO levels at the Moody Tower (MT) site close to downtown were dependent on the wind direction: southerly maritime winds brought in background levels (0.5–1 ppbv) while trajectories originating in the HSC resulted in high HCHO (up to 31.5 ppbv). Based on the best multiparametric linear regression model fit, the HCHO levels at the MT site can be accounted for as follows: 38.5±12.3% from primary vehicular emissions (using CO as an index of vehicular emission), 24.1±17.7% formed photochemically (using peroxyacetic nitric anhydride (PAN) as an index of photochemical activity) and 8.9±11.2% from industrial emissions (using SO_2 as an index of industrial emissions). The balance 28.5±12.7% constituted the residual which cannot be easily ascribed to the above categories and/or which is transported into the HGA. The CO related HCHO fraction is dominant during the morning rush hour (06:00–09:00 h , all times are given in CDT); on a carbon basis, HCHO emissions are up to 0.7% of the CO emissions. The SO_2 related HCHO fraction is significant between 09:00–12:00 h. After 12:00 h HCHO is largely formed through secondary processes. The HCHO/PAN ratios are dependent on the SO_2 levels. The SO_2 related HCHO fraction at the downtown site originates in the ship channel. Aside from traffic-related primary HCHO emissions, HCHO of industrial origin serves as an appreciable source for OH in the morning.

ACPD

9, 24193–24223, 2009

1 Introduction

The Houston Galveston Airshed (HGA) continues to be a non-attainment region under United States federal ozone standards. Rapid ozone (O_3) formation processes are associated with releases of highly reactive volatile organic compounds (HRVOCs) from industrial facilities predominantly located in Houston's Ship Channel (HSC), which comprise large agglomerations of petrochemical industries (Kleinman et al., 2002; Daum et al., 2003, 2004; Ryerson et al., 2003; Berkowitz et al., 2005); the impact of non methane hydrocarbons on downwind non-industrialized areas has been extensively studied (Leuchner and Rappenglück, 2009). Among HRVOCs compounds that serve as radical sources are of particular concern. Formaldehyde (HCHO) is considered to be an important radical precursor through photolytic formation of HCO· and H· that then variously lead to HO_2· and ·OH radicals.

While HCHO may be emitted primarily from incomplete combustion in either mobile or stationary sources (Zweidinger et al., 1988; Altshuller, 1993; Chen et al., 2004; Dasgupta et al., 2005), it can also be formed from ozonolysis of terminal olefins, a pathway that does not consume OH. Relatively stable at night, HCHO rapidly photolyzes after sunrise and serves as an important source for early morning radicals.

Some of the highest HCHO levels in North America have been reported for the HGA, in particular the HSC area, ranging from ~35 to 52 ppbv (Dasgupta et al., 2005; Eom et al., 2008). Airborne HCHO measurements in HGA likewise exceeded 30 ppbv on some occasions; terminal olefins were identified as the most important precursors (Wert et al., 2003). In the HSC, HCHO events, e.g. short-term increases of HCHO mixing ratios up to 15 ppbv during nighttime, have been reported to coincide with SO_2 and H_2O_2 excursions, suggesting that HRVOCs may be co-emitted with SO_2 from specific sources and lead to rapid production of peroxy radicals (Dasgupta et al., 2005). The same study also reported nighttime excursions of HCHO, possibly from flare combustion (the events were accompanied by NO peaks); primary HCHO is thus likely present in at least some industrial emissions.

ACPD
9, 24193–24223, 2009

Several previous studies in various urban areas (Anderson et al., 1996; Possanzini et al., 1996; Friedfeld et al., 2002; Possanzini et al., 2002; Rappenglück et al., 2005; Garcia et al., 2006) estimated contributions of primary emissions to the observed HCHO; up to 37% was estimated for the HGA (Friedfeld et al., 2002). The primary HCHO fraction originating from traffic emissions showed strong diurnal variation (Rappenglück et al., 2005; Garcia et al., 2006) with morning rush hour maxima (up to 100%) and midday minima (down to 20%) as insolation intensity reached a maximum.

In August–September 2006, we made continuous measurements of HCHO and other gases on the University of Houston (UH) Moody Tower (MT). With the help of two other continuous HCHO measurement sites in the HSC area, we decipher and discuss the potential HCHO sources in the HGA.

2 Methods

The MT site (lat./long. 29.717639°/−95.341250°, 4 km southeast of downtown Houston (see Fig. 1) is 60 m above ground level in the 2.2 km^2 UH campus: all other campus buildings are substantially lower in height. Meteorological as well as air chemistry data were collected from a 12-m high sampling tower installed on the top of MT from 18 August 2006–15 October 2006. The site is sufficiently removed from the impact of local surface emissions and is well-suited for assessing photochemical processing in the HGA boundary layer. Formaldehyde was measured using the fluorometric Hantzsch reaction (FHR, model AL4021, http://www.aerolaser.com). Other custom instrumentation based on the same FHR chemistry (Eom et al., 2008) were deployed at US Environmental Protection Agency (USEPA) site number 48-201-0803, Houston, TX (HRM-3, lat/long.: 29.765278°/−95.181111°) and at USEPA site number 48-201-1015, Baytown, TX (LF, Lynchburg Ferry, lat/long.: 29.764444°/−95.077778°), both near the HSC (Fig. 1). These sites provided HCHO data from 22 August 2006–14 October 2006.

FHR based HCHO measurement instrumentation have been extensively field-used and validated (Gilpin et al., 1997; Cárdenas et al., 2000; Klemp et al., 2003; Hak et al.,

ACPD
9, 24193–24223, 2009

2005; Apel et al., 2008; Wisthaler et al., 2008). The limit of detection for the three HCHO instruments ranged from 50–120 pptv (three times signal-to-noise ratio); the estimated uncertainty was ~10%. Absolute calibration was performed with aqueous standards monthly or with solution change; an on-board permeation source was used for daily calibration; instruments were also zeroed daily. Data for HRVOC's were obtained by using automated gas chromatography – flame ionization detection (Leuchner and Rappenglück, 2009). At the MT site, CO, SO_2, and oxides of nitrogen (NO, NO_2, NO_x) were also determined using methods outlined in Luke et al., (2007 and 2009). PAN was measured using a modified Metcon gas chromatograph coupled to an electron capture detector, GC/ECD). At all sites, basic meteorological measurements were made.

3 Results and discussion

3.1 General observations

The high, mean (median) concentrations at the MT, HRM3 and LF sites, respectively were 32.5, 3.4 (2.9); 31.5, 4.4 (3.6); and 52.4, 7.1 (6.6) ppbv. A statistical summary is given in Table 1. The LF site typically exhibited the highest mixing ratios. The mean median and standard deviation of diurnal variations of HCHO are shown in Fig. 2. The mixing ratios at HRM3 and LF are higher than those at MT, especially during daytime periods; also, the mean LF HCHO levels were 2–3 ppbv higher than others. In contrast to the HSC sites, median HCHO levels at MT show a peak in the median values during the morning hours (06:00–10:00 h) likely indicating rush hour impact. Figure 3 displays the MT HCHO data separated into "urban" and "HSC" wind sectors (see Fig. 1). The two peaks in the MT(urban) data, morning rush hour and the mid-afternoon, are of similar magnitude. The MT(HSC) concentrations are up to three times higher and approach the LF levels. The MT(urban) and MT(HSC) levels are similar only briefly around 16:00 h, usually coinciding with the diurnal maximum height of the boundary

ACPD
9, 24193–24223, 2009

layer during this field campaign (Rappenglück et al., 2008) and thus with the peak atmospheric mixing period. The MT(HSC) diurnal maximum occurs between the two MT(urban) HCHO peaks. The standard deviation (Fig. 2) is an indicator of short term HCHO events; this is highest for LF. For all sites, the highest standard deviation occurs during 10:00–13:00 h; this is the same period when HCHO levels generally peak at all the sites (Figs. 2 and 3). During the morning rush hour at MT, it is notable that the absolute standard deviation is low despite high HCHO levels, reflecting traffic emissions that are reproducible on a day to day basis.

In an approach to explore the presence of primary HCHO we split the HCHO data set into daytime (defined as 09:00–21:00 h) and nighttime (21:00–09:00 h) values. "Nighttime" as defined in this case would include some hours of early daylight in the morning, but this time period was selected based on a combination of criteria: (1) limited solar radiation, (2) limited turbulent and convective atmospheric mixing, (3) likelihood of low boundary layer heights (e.g., Rappenglück et al., 2008; Day et al., 2009), and (4) the presence of rush hour emissions. This selection would most likely include time periods with the maximum fraction of primary HCHO in ambient HCHO. In fact we carried out the same study for nighttime periods excluding the timeframe 07:00–09:00 h, i.e. without major parts of the morning rush hour and actually found slightly higher HCHO/CO ratios. We believe that this may be due to some non negligible remnants of HCHO which was photochemically produced the day before.

Figure 4 displays HCHO daytime and nighttime wind roses for all sites. Daytime and nighttime median values are quite similar for each site. This holds for the spatial distribution as well as for the absolute amount of HCHO mixing ratios. The minima occur at night with southerly wind; this is the same for minima of other primarily emitted anthropogenic trace gases such as acetylene (not further discussed here). HCHO levels of 0.5–1 ppbv are observed at MT under these conditions, we take this range to be representative of background air masses coming from the Gulf of Mexico.

Median nighttime values at LF are comparable to those at daytime (~8 ppbv); for W-NW wind, nighttime median values exceed daytime median values (Fig. 4). At MT,

ACPD
9, 24193–24223, 2009

daytime and nighttime maximum median values are associated with E and NE winds (5–6.5 ppbv); the HSC is ENE of MT. For HRM3 higher nighttime median values are mainly associated with three sectors: NNE-NE (3.5–4.1 ppbv), ESE-SE (3.4–3.6 ppbv), and SW (~4.6 ppbv). Maximum values also show some distinct dependencies on wind direction. It should be noted that nighttime maximum values can reach about 17 ppbv at the LF site and between 10–15 ppbv at the other sites. These findings suggest some relation to small scale plume events. The observed nighttime HCHO may be primary or originates from ozone-olefin reactions.

3.2 Possible contributions to ambient HCHO levels

CO originates exclusively from combustion; CO has previously been used as an index of vehicular emissions (Anderson et al., 1996; Possanzini et al., 1996; Friedfeld et al., 2002; Garcia et al., 2006; Rappenglück et al., 2005). This ratio is typically 0.001–0.002 for gasoline engine passenger cars but can be 10× higher for diesel cars (Schmitz et al., 1999); in all cases this strongly depends on driving conditions that can substantially influence CO and/or HCHO emission per unit carbon consumed (Herndon et al., 2007) and motor vehicle fuel oxygenate composition. Consequently, HCHO/CO ratio may vary with the sampling location. In addition, it will be modified when secondary production of HCHO occurs during the daytime.

At MT, CO mixing ratios are largely independent of wind direction, except that distinct minima (about 50% less than the average median values) are always observed with southerly maritime wind (see Fig. 5); traffic emissions therefore contribute the same way for MT(urban) and MT(HSC) wind sectors.

The HCHO−CO relationships for MT(urban) and MT(HSC) are shown in Fig. 6. By far the best HCHO−CO correlation (linear r^2=0.66) is for nighttime MT(urban) (this includes much of the morning rush hour) with a slope of 7.1 pptv HCHO/ppbv CO. The next best correlated data, the nighttime MT(HSC) data, exhibit a slope of 5.2 pptv HCHO/ppbv CO, with a much poorer linear r^2 of 0.23, indicating weak dependencies. MT(urban) daytime data has a slope 6.4 pptv HCHO/ppbv CO, similar to the nighttime

ACPD
9, 24193–24223, 2009

slope at that location albeit correlation is weaker still (r^2=0.20). MT(HSC) daytime data show little correlation (r^2=0.13). Weaker correlations during the daytime are most likely due to the importance of daytime photochemistry leading to varying amount of HCHO. Based on the MT nighttime data sets we thus estimate the upper limit for traffic related primary HCHO emissions to be 0.5–0.7% of the CO emissions.

Previous studies have used CO for estimating the primary HCHO fraction. For estimating secondary HCHO fractions either ozone (Friedfeld et al., 2002) or glyoxal (CHOCHO) (Garcia et al., 2006) were used. In our study we apply multiple surrogates for HCHO: (i) CO as a surrogate for vehicular source, (ii) PAN as an unambiguous photochemical tracer (in contrast to ozone, HCHO is not among the precursors for PAN, formation of PAN is not related to HCHO chemistry) and (iii) SO_2 as an indicator for industrial sources. PAN is a likely better surrogate for photochemical processes than ozone, since (i) background concentrations of PAN are negligible and (ii) PAN is not a priori related to HCHO. Based on the MT data set (it offered the most complete trace gas data sets among the three sites) we obtained the following best fit equation (using the least squares fitting routine in Microsoft Excel Solver™ (Dasgupta, 2008), and the *Solveraid* approach (de Levie, 2004) to calculate 95% uncertainty bounds):

$$[\mathrm{HCHO}] = (5.55 \pm 0.40) \times 10^{-3}[\mathrm{CO}] + 1.88 \pm 0.06[\mathrm{PAN}] + 0.172 \pm 0.008[\mathrm{SO_2}] + 0.857 \pm 0.107, r^2 = 0.80 \quad (1)$$

where all concentrations are in ppbv. The intercept represents residual HCHO that cannot be accounted for by the above sources and likely represents a mixture of both secondary and primary HCHO. It may also include transport from areas outside the HGA. We checked the usefulness of additionally incorporating ethylene as a marker of flare emissions; however, this did not significantly improve the fit (r^2=0.81) and was not further pursued. On the other hand, the correlation dropped markedly (r^2=0.64) if the SO_2 term was omitted.

ACPD
9, 24193–24223, 2009

3.3 Illustrative examples for regression model fit

We consider here two separate periods; in both cases the data spans from near background values to a significant excursion. On 14 September 2006 the overnight HCHO background at MT is <5 ppbv at 02:00 h (Fig. 7a), beginning at ~08:00 h, the HCHO concentration begins rising and reaches a peak of 32.5 ppbv at 11:40 h. The rise in HCHO is accompanied by excursions of SO_2, ethylene, and PAN. There is a slight decrease in CO. The prediction agrees very well with the observed values as shown in Fig. 7b which also depicts the contributions of each of the terms in Eq. (1); it also portrays the diurnal change in the relative contributions of each of the parameters.

The HCHO excursion on 29 September (Fig. 8a) peaks even earlier in the morning, between 09:30–10:00 h. A backward trajectory analysis using the University of Houston Real-time Interactive Trajectory System (Byun et al., 2004) (Fig. 9) shows the air mass came directly from the HSC area to MT. Both SO_2 and PAN (and NO; not shown) show peak values essentially coincident with the HCHO excursion, while CO and C_2H_4, both of which were high prior to the HCHO peak, begins to decrease as the HCHO peak begins to subside. The fact that CO levels abruptly decrease during this time suggests that transport from the HSC area may also be impacted by the break-up of the morning inversion that may have resulted in downward mixing of any SO_2, HCHO, and PAN present in layers aloft. Tethersonde data (Day et al., 2009) suggest low nocturnal boundary layers (100–200 m agl) in the HGA; radiosonde data at 07:00 h on that day also indicates a boundary layer height of ≤200 m agl. There have been indications for stratified SO_2 plumes aloft based on early morning ozone sonde launchings (Rappenglück et al., 2008), others have previously observed simultaneously elevated SO_2 and HCHO at HSC (Dasgupta et al., 2005), possibly related to refinery flare emissions or emissions from collocated facilities. It is possible that this plume of high early morning HCHO may originate from hot plumes that penetrate the nocturnal and early morning boundary layer. Whatever the exact origin, the regression model predictions also agree reasonably well with the observed HCHO levels prior to

ACPD
9, 24193–24223, 2009

and during the excursion, albeit the post excursion values in the afternoon and continuing into the evening and night are somewhat over-predicted by the regression model. Both events have in common that the HCHO/PAN ratios were higher by >2× during the HCHO events relative to subsequent afternoon hours.

3.4 HCHO/PAN ratio and SO_2

We observe that when the HCHO and PAN data for the MT(HSC) wind sector are plotted against each other, they fall in three classes that largely depend on the SO_2 concentration (Fig. 10). For <20 ppbv SO_2 (blue and green symbols in Fig. 10), HCHO is always <15 ppbv, more than 90% of the time it is <10 ppbv (blue symbols in Fig. 10). For <10 ppbv SO_2, the PAN levels are linearly correlated with HCHO (r^2=0.51, slope 1.54 ppbv HCHO/ppbv PAN). Similar values are obtained for MT(urban). However, MT(urban) SO_2 levels never exceeded 10 ppbv and this aspect will therefore will not be further discussed. While the data group indicated by the green symbols (SO_2 levels between 10–20 ppbv) in Fig. 10 is somewhat less correlated, the third group represented by red dots shows stronger linear correlation (r^2=0.86, slope 4.36 ppbv HCHO/ppbv PAN). This group consists of samples with SO_2 concentrations 20–60 ppbv with a few containing 60+ppbv SO_2. The different slope values are consistent with the observation that HCHO events are accompanied by significantly higher HCHO/PAN ratios. The possibilities include: (i) some primary HCHO is associated with SO_2 emitting sources and (ii) VOCs that react to form both HCHO and PAN are (a) co-emitted with SO_2 and/or (b) emitted from sources collocated to SO_2 emission sources. The correlation between HCHO and PAN is both significant and bimodal; this suggests at least two different types of VOCs that are being emitted. For instance, photochemical degradation of ethylene would lead to the formation of HCHO but not PAN, whereas propylene would be able to serve as a precursor for both HCHO and PAN.

ACPD
9, 24193–24223, 2009

3.5 Overall contributions

As shown in the insets of Figs. 7b and 8b, we can evaluate the fraction of HCHO associated with each surrogate. Considering all days, the HCHO levels at the MT site can be accounted for as follows: 38.5±12.3% from primary vehicular emissions (using CO as an index; this is slightly higher than the 37% previously suggested (Friedfeld et al., 2002), 24.1±17.7% formed photochemically (using PAN as an index) and 8.9±11.2% from industrial emissions (using SO_2 as an index). The balance 28.5±12.7% constituted the residual which cannot be easily ascribed to the above categories and/or which is transported into the HGA. All fractions show distinct diurnal variations that are closely linked to the diurnal variations of emissions, photochemical processes and wind patterns (see Figs. 7b and 8b): The primary HCHO is dominant in the morning rush hour (06:00–09:00 h); the SO_2 related HCHO fraction, which occurs under wind directions from the HSC, prevails between 09:00–12:00 h. In the afternoon HCHO is dominantly of secondary origin. Residual HCHO shows only limited diurnal variation. On an hourly basis, the range of the fractions are: CO-related HCHO (8.9–74.8%), PAN-related HCHO (1.7%–70.8%.), SO_2 related HCHO (0.1–67.2%), and residual HCHO (3.5–60.8%).

The SO_2 related HCHO fraction as well as residual HCHO have a strong dependence on wind direction (Fig. 11) and thus their diurnal variations are controlled by local wind systems, e.g. the land sea breeze system, which favors morning transport of polluted air masses from the Ship Channel, or synoptic conditions which often provide persistent southerly winds and advect unpolluted marine air masses (Rappenglück et al., 2008). The SO_2 fraction displays a distinct maximum under E-ENE wind, (also SW during daytime) and more importantly under E-NNE wind during nighttime, suggesting point sources. Median SO_2-related HCHO fraction for these wind directions can reach 20–30% during daytime (average median fraction: 6.2%) and up to 40% at nighttime (average median fraction: 10.1%). While the absolute median value of HCHO is low (1.2–2.0 ppb), the fractional contribution of residual HCHO is maximal

ACPD
9, 24193–24223, 2009

(between ≈47–50%) when marine winds come in, suggesting background air masses.

3.6 Dependence on wind direction

Figure 12 displays contributions to ambient HCHO mixing ratios and their dependence on wind direction. In addition, median mixing ratios of selected olefins are included. Background HCHO contributions range from 500 pptv–1 ppbv and show the least directional dependence. Under "urban" and HSC wind directions, the secondary HCHO fraction exceeds the primary HCHO fraction during the day. At night, the primary HCHO fraction dominates. As can be seen for the daytime data, the wind roses for ethylene and propylene largely correlate with the non-CO HCHO fraction, suggesting OH driven photochemistry during daytime. As mentioned before, the SO_2 fraction plays a distinct role under very specific wind directions, predominantly coming from the HSC area. While mixing ratios of ethylene and propylene seem to better correlate with the PAN-related HCHO fraction than the SO_2 related fraction during the daytime, they show a closer relationship with the SO_2-related fraction during nighttime. In all cases, propylene correlates better than ethylene with the SO_2-related fraction, displaying a maximum r^2=0.94 during nighttime. This close relationship either implies co-emission of HCHO or HCHO formation through ozonolysis of alkenes during nighttime. Though the simultaneous occurrence of PAN may hint exclusively to secondary production of HCHO, the possibility that other processes may be co-occurring cannot be excluded.

At the MT site, after the breakdown of the morning inversion, there are frequently excursions of HCHO, together with those of SO_2 and PAN; the SO_2 related HCHO fraction observed at MT is distinctively linked to trajectories passing the highly industrialized HSC area. Apart from traffic-related primary vehicular HCHO emissions, industrial releases of HCHO may be non-negligible in the HGA and may serve as an appreciable source for OH in the early morning.

ACPD
9, 24193–24223, 2009

4 Conclusions

In-situ measurements of formaldehyde performed in Houston, Texas, in summer 2006 showed a wide dynamic range. At the Moody Tower site close to the downtown area of Houston HCHO was found to correlate with PAN, indicating photochemical formation, with CO, indicating primary traffic related sources, and with SO_2, indicating industry related impacts. On a carbon basis, HCHO emissions from mobile sources are up to 0.7% of the corresponding CO emissions. This HCHO fraction is dominant during the morning rush hour (06:00–09:00 h). The SO_2 related HCHO fraction occurs between 09:00–12:00 h. After 12:00 h HCHO is largely of secondary origin. HCHO/PAN ratios depend on SO_2 levels. The SO_2 related HCHO fraction at the Moody Tower site is distinctively linked to trajectories passing the industrial Ship Channel area. Apart from traffic-related primary HCHO emissions, industrial releases of HCHO may be non-negligible and may serve as an appreciable source for OH in the morning.

Acknowledgements. The authors would like to thank the Houston Advanced Research Center (HARC) and Texas Commission on Environmental Quality (TCEQ) for their support. Special thanks to L. Pedemonte and J. Massingale for working on VOC data reduction as well as to B. Lefer and J. Flynn for the MT wind data. Backward trajectory analysis was provided by B. Czader using the Real-time Interactive Trajectory System.

References

Altshuller, A. P.: Production of aldehydes as primary emissions and from secondary atmospheric reactions of alkenes and alkanes during the night and early morning hours, Atmos. Environ., 27A, 21–32, 1993.

Anderson, L. G., Lanning, J. A., Barrell, R., Miygishima, J., Jones, R. H., and Wolfe, P.: Sources and sinks of formaldehyde and acetaldehyde: an analysis of Denver's ambient concentration data, Atmos. Environ., 30, 2113–2123, 1996.

Apel, A. C., Brauers, T., Koppmann, R., Bandowe, B., Boßmeyer, J., Holzke, C., Tillmann, R., Wahner, A., Wegener, R., Brunner, A., Jocher, M., Ruuskanen, T., Spirig, C.,

Steigner, D., Steinbrecher, R., Gomez Alvarez, E., Müller, K., Burrows, J. P., Schade, G., Solomon, S. J., Ladstätter-Weißenmayer, A., Simmond, P., Young, D., Hopkins, J. R., Lewis, A. C., Legreid, G., Reimann, S., Hansel, A., Wisthaler, A., Blake, R. S., Ellis, A. M., Monks, P. S., and Wyc, K. P.: Intercomparison of oxygenated volatile organic compound (OVOC) measurements at the SAPHIR atmosphere simulation chamber, J. Geophys. Res., 113, D20307, doi:10.1029/2008JD009865, 2008.

Berkowitz, C. M., Spicer, C. W., and Doskey, P. V.: Hydrocarbon observations and ozone production rates in Western Houston during the Texas 2000 Air Quality Study, Atmos. Environ., 39, 3383–3396, 2005.

Byun, D. W., Kim, S.-B., Moon, N.-K., Ngan, F., Li, Y., Ng, T.: Real-Time Trajectory Analysis Operation and Tool Development Project H-10-2003 Final Report, Texas Environmental Research Consortium, Houston, TX, 2004.

Cárdenas, L. M., Brassington, D. J., Allen, B. J., Coe, H., Alicke, B., Platt, U., Wilson, K. M., Plane, J. M. C., and Penkett, S. A.: Intercomparison of formaldehyde measurements in clean and polluted atmospheres, J. Atmos. Chem., 37, 53–80, 2000.

Chen, J., So, S., Lee, H., Fraser, M. P., Curl, R. F., Harman, T., and Tittel, F. K.: Atmospheric formaldehyde monitoring in the greater Houston area in 2002, Appl. Spectrosc., 58, 243–247, 2004.

Dasgupta, P. K., Li, J., Zhang, G., Luke, W. T., McClenny, W. A., Stutz, J., and Fried, A.: Summertime ambient formaldehyde in five U.S. metropolitan areas: Nashville, Atlanta, Houston, Philadelphia, and Tampa, Environ. Sci. Technol., 39, 4767–4783, 2005.

Dasgupta, P. K.: Chromatographic peak resolution using Microsoft Excel Solver. The merit of time shifting input arrays, J. Chromatogr. A, 1213, 50–55, 2008.

Daum, P. H., Kleinman, L. I., Springston, S. R., Nunnermacker, L. J., Lee, Y.-N., Weinstein-Lloyd, J., Zheng, J., and Berkowitz, C.: A comparative study of O_3 formation in the Houston urban and industrial plumes during the TEXAQS 2000 study, J. Geophys. Res., 108, 4715, doi:10.1029/2003JD003552, 2003.

Daum, P. H., Kleinman, L. I., Springston, S. R., Nunnermacker, L. J., Lee, Y.-N., Weinstein-Lloyd, J., Zheng, J., and Berkowitz, C.: Origin and properties of plumes of high ozone observed during Texas 2000 Air Quality Study (TEXAQS 2000), J. Geophys. Res., 109, D17306, doi:10.1029/2003JD004311, 2004.

Day, B. M., Rappenglück, B., Clements, C. B., Tucker, S. C., and Brewer, W. A.: Nocturnal boundary layer characteristics and land breeze development in Houston, Texas, during

TexAQS-II, Atmos. Environ., doi:10.1016/j.atmosenv.2009.01.031, in press, 2009.
de Levie, R.: Advanced Excel for Scientific Data Analysis, Oxford University Press, 2004.
Eom, I.-Y., Li, Q., Li, J., and Dasgupta, P.: Robust hybrid flow analyzer for formaldehyde, Environ. Sci. Technol., 42, 1221–1226, 2008.
Friedfeld, S., Fraser, M., Ensor, K., Tribble, S., Rehle, D., Leleux, D., and Tittel, F.: Statistical analysis of primary and secondary atmospheric formaldehyde, Atmos. Environ., 36, 4767–4775, 2002.
Garcia, A. R., Volkamer, R., Molina, L. T., Molina, M. J., Samuelson, J., Mellqvist, J., Galle, B., Herndon, S. C., and Kolb, C. E.: Separation of emitted and photochemical formaldehyde in Mexico City using a statistical analysis and a new pair of gas-phase tracers, Atmos. Chem. Phys., 6, 4545–4557, 2006
Gilpin, T., Apel, E., Fried, A., Wert, B., Calvert, J., Genfa, Z., Dasgupta, P. K., Harder, J. W., Heikes, B. G., Hopkins, B., Westberg, H., Kleindienst, T., Lee, Y.-N., Zhou, X., Lonneman, W., and Sewell, S.: Intercomparison of six ambient [CH_2O] measurement techniques, J. Geophys. Res., 102, 21161–21188, 1997.
Hak, C., Pundt, I., Trick, S., Kern, C., Platt, U., Dommen, J., Ordóñez, C., Prévôt, A. S. H., Junkermann, W., Astorga-Llorns, C., Larsen, B. R., Mellqvist, J., Strandberg, A., Yu, Y., Galle, B., Kleffmann, J., Lörzer, J. C., Braathen, G. O., and Volkamer, R.: Intercomparison of four different in-situ techniques for ambient formaldehyde measurements in urban air, Atmos. Chem. Phys., 5, 2881–2900, 2005, http://www.atmos-chem-phys.net/5/2881/2005/.
Herndon, S. C., Zahniser, M. S., Nelson Jr., D. D., Shorter, J., McManus, J. B., Jiménez. R., Warneke, C., and de Gouw, J. A.: Airborne measurements of HCHO and HCOOH during the New England Air Quality Study 2004 using a pulsed quantum cascade laser spectrometer, J. Geophys. Res., 112, D10S03, doi:10.1029/2006JD007600, 2007.
Kleinman, L. I., Daum, P. H., Imre, D., Lee, Y.-N., Nunnermacker, L. J., Springston, S. R., Weinstein-Lloyd, J., and Rudolph, J.: Ozone production rate and hydrocarbon reactivity in 5 urban areas. A cause of high ozone concentrations in Houston, Geophys. Res. Lett., 29, 1467, doi:10.1029/2001GL014569, 2002, Correction: 30, 1639, doi:10.1029/2003GL017485, 2004.
Klemp, D., Mannschreck, K., and Mittermaier, B.: Comparison of two different HCHO measurement techniques: TDLAS and a commercial Hantzsch monitor – results from long-term measurements in a city plume during the EVA experiment, in: Emissions of Air Pollutants – Mea-

surements, Calculations and Uncertainties, edited by: Friedrich, R. and Reis, S., Springer Verlag, Berlin Heidelberg, 2003.
Leuchner, M. and Rappenglück, B.: VOC Source-Receptor Relationships in Houston during TexAQS-II, Atmos. Environ., doi:10.1016/j.atmosenv.2009.02.029, in press, 2009.
Luke, W.T, Kelley, P., Lefer, B. L., Flynn, J., Rappenglück, B., Leuchner, M., Dibb, J. E., Ziemba, L. D., Anderson, C. H., and Buhr, M. P.: Measurements of primary trace gases and NO_y speciation during TRAMP, Atmos. Environ., doi:10.1016/j.atmosenv.2009.08.014, in press, 2009.
Luke, W. T., Arnold, J. R., Gunter, R. L., Watson, T. B., Wellman, D. L., Dasgupta, P. K., Li, J., Riemer, D., and Tate, P.: The NOAA Twin Otter and its role in BRACE: platform description, Atmos. Environ., 41, 4177–4189, 2007.
Possanzini, M., Di Palo, V., and Cecinato, A.: Sources and photodecomposition of formaldehyde and acetaldehyde in Rome ambient air, Atmos. Environ., 36, 3195–3201, 2002.
Possanzini, M., Di Palo, V., Petricca, M., Fratarcangeli, R., and Brocco, D.: Measurements of lower carbonyls in Rome ambient air, Atmos. Environ., 30, 3757–3764, 1996.
Rappenglück, B., Perna, R., Zhong, S., and Morris, G. A.: An analysis of the vertical structure of the atmosphere and the upper-level meteorology and their impact on surface ozone levels in Houston, Texas, J. Geophys. Res., 113, D17315, doi:10.1029/2007JD009745, 2008.
Rappenglück, B., Schmitz, R., Bauerfeind, M., Cereceda-Balic, F., v. Baer, D., Jorquera, H., Silva, Y., and Oyola, P.: An urban photochemistry study in Santiago de Chile, Atmos. Environ., 39, 2913–2931, 2005.
Ryerson, T. B., Trainer, M., Angevine, W. M., Brock, C. A., Dissly, R. W., Fehsenfeld, F. C., Frost, G. J., Goldan, P. D., Holloway, J. S., Hübler, G., Jakoubek, R. O., Kuster, W. C., Neuman, J. A., Nicks Jr., D. K., Parrish, D. D., Roberts, J. M., Sueper, D. T., Atlas, E. L., Donnelly, S. G., Flocke, F., Fried, A., Potter, W. T., Schauffler, S., Stroud, V., Weinheimer, A. J., Wert, B. P., Wiedinmyer, C., Alvarez, R. J., Banta, R. M., Darby, L. S., and Senff, C. J.: Effect of petrochemical industrial emissions of reactive alkenes and NO_x on tropospheric ozone formation in Houston, Texas, J. Geophys. Res., 108, 4249, doi:10.1029/2002JD003070, 2003.
Schmitz, T., Hassel, D., and Weber, F. J.: Zusammensetzung der Kohlenwasserstoffe im Abgas unterschiedlicher Abgaskonzepte. Berichte des Forschungszentrums Jülich, JÜL-3646, 1999.
Springston, S. R., Kleinman, L. I., Brechtel, F., Lee, Y.-N., Nunnermacker, L. J., and Wang, J.: Chemical evolution of an isolated power plant plume during the TexAQS 2000 study, Atmos.

Environ., 39, 3431–3443, 2005.
Wert, B. P., Trainer, M., Fried, A., Ryerson, T. B., Henry, B., Potter, W., Angevine, W. M., Atlas, E., Donnelly, S. G., Fehsenfeld, F. C., Frost, G. J., Goldan, P. D., Hansel, A., Holloway, J. S., Hubler, G., Kuster, W. C., Nicks Jr., D. K., Neuman, J. A., Parrish, D. D., Schauffler, S., Stutz, J., Sueper, D. T., Wiedinmyer, C., and Wisthaler, A.: Signatures of terminal alkene oxidation in airborne formaldehyde measurements during TexAQS 2000, J. Geophys. Res., 108, 4104, doi:10.1029/2002JD002502, 2003.
Wisthaler, A., Apel, E. C., Bossmeyer, J., Hansel, A., Junkermann, W., Koppmann, R., Meier, R., Müller, K., Solomon, S. J., Steinbrecher, R., Tillmann, R., and Brauers, T.: Technical Note: Intercomparison of formaldehyde measurements at the atmosphere simulation chamber SAPHIR, Atmos. Chem. Phys., 8, 2189–2200, 2008, http://www.atmos-chem-phys.net/8/2189/2008/.
Zweidinger, R. B., Sigsby, J. E., Tejada, S. B., Stump, F. D., Dropkin, D. L., Ray, W. D., and Duncan, J. W.: Detailed hydrocarbon and aldehyde mobile source emissions from roadway studies, Environ. Sci. Technol., 22, 956–962, 1988.

Table 1. Statistical data for HCHO measurements at the MT, HRM3, and LF site based on 10-min data.

	MT	HRM3	LF
# Measurements	5344	5239	6207
Maximum [ppbv]	32.54	31.53	52.44
Mean [ppbv]	3.41	4.39	7.10
Median [ppbv]	2.88	3.55	6.62

ACPD
9, 24193–24223, 2009

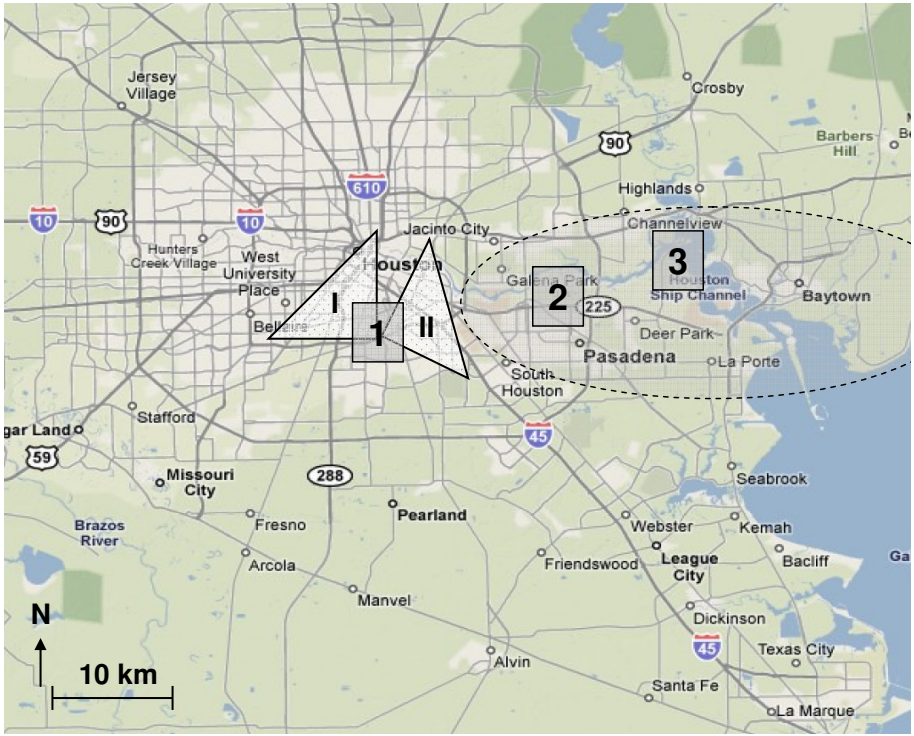

Fig. 1. HCHO measurement sites: MT (1), HRM3 (2), and LF site (3). The highlighted area indicates the HSC area. Sectors (I) and (II) at the MT designate wind directions which either point to "urban" (wind direction between 270°–360°) or "HSC" (wind direction between 22.5°–112.5°) source areas (corresponding discussion see text).

ACPD
9, 24193–24223, 2009

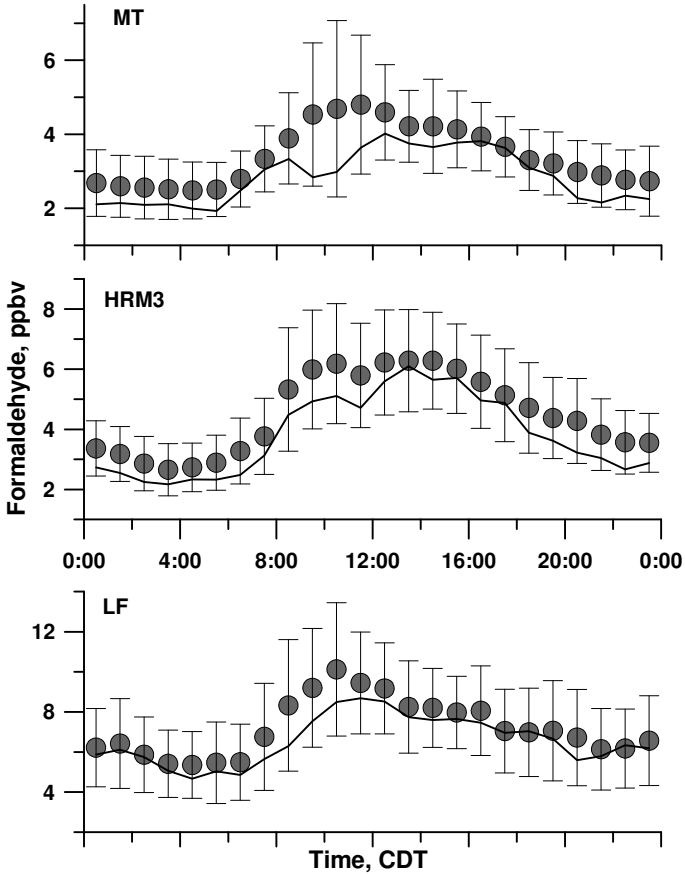

Fig. 2. Composite diurnal variation of hourly data of the median (solid line) and mean (circles, with the error bars spanning 1 standard deviation) of formaldehyde mixing ratios obtained at the MT, HRM3, and LF sites. Note different ordinate scaling in the three panels.

ACPD
9, 24193–24223, 2009

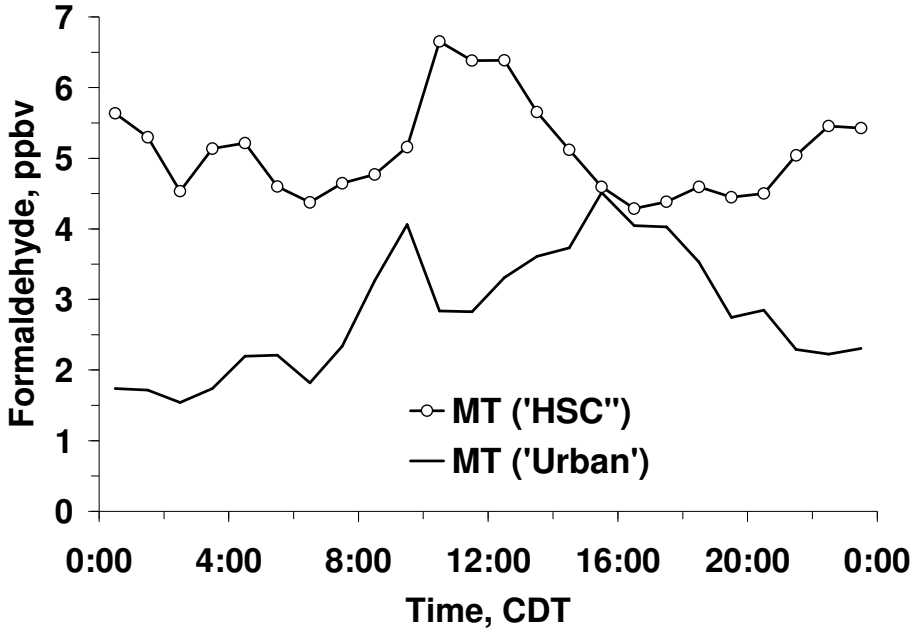

Fig. 3. Composite diurnal variations of formaldehyde at the Moody Tower for the "Urban" and the "Houston Ship Channel" sector. Designations "Urban" and "HSC" are defined as shown in Fig. 1. Only cases with wind speeds >0.5 m/s were considered. Median values are shown.

ACPD
9, 24193–24223, 2009

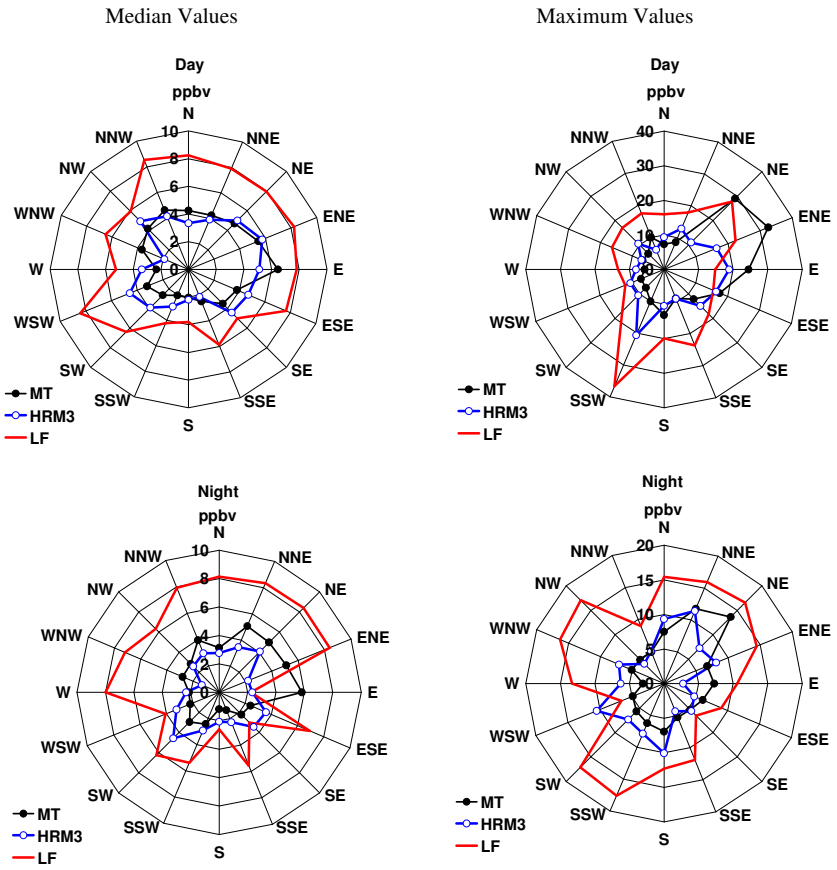

Fig. 4. Formaldehyde pollution roses for the Moody Tower, HRM3, and the Lynchburg Ferry site based on hourly averages (left column: median values; right column: maximum values). Nighttimes are defined as 21:00–09:00 h and daytimes as 09:00–21:00 h (see also text).

ACPD
9, 24193–24223, 2009

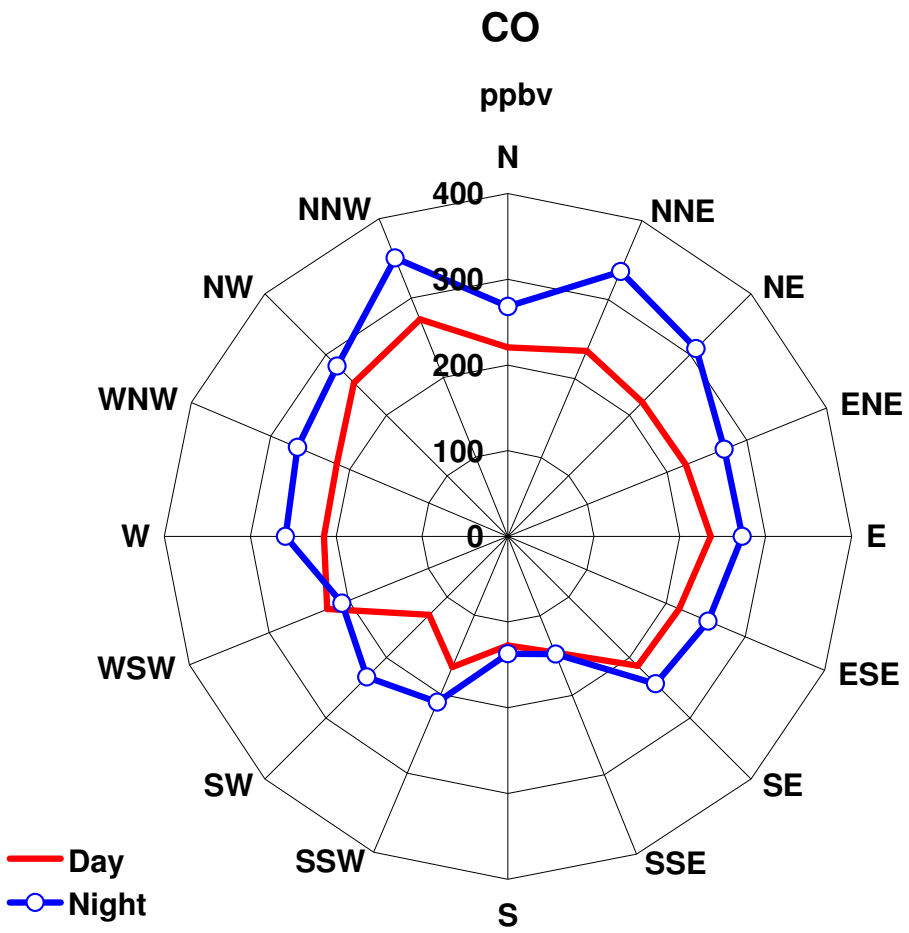

Fig. 5. CO pollution roses for the MT based on hourly averages. Night- and daytimes defined as in Fig. 4.

ACPD
9, 24193–24223, 2009

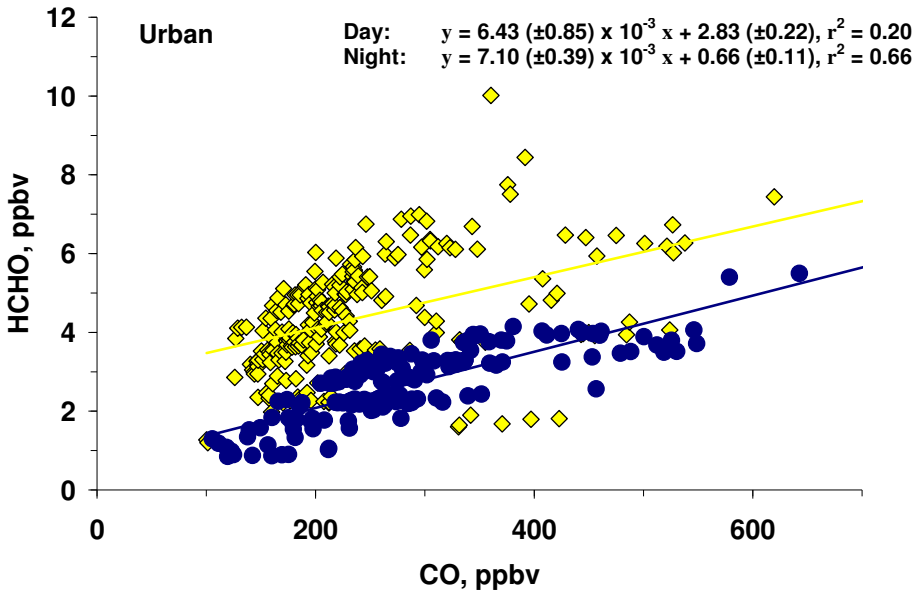

Fig. 6a. Relationships of HCHO to CO obtained at the MT. Designation "Urban" is defined the same way as for Fig. 1. Yellow diamonds represent daytime measurements, blue dots represent nighttime measurements. Night- and daytimes defined as in Fig. 4.

ACPD
9, 24193–24223, 2009

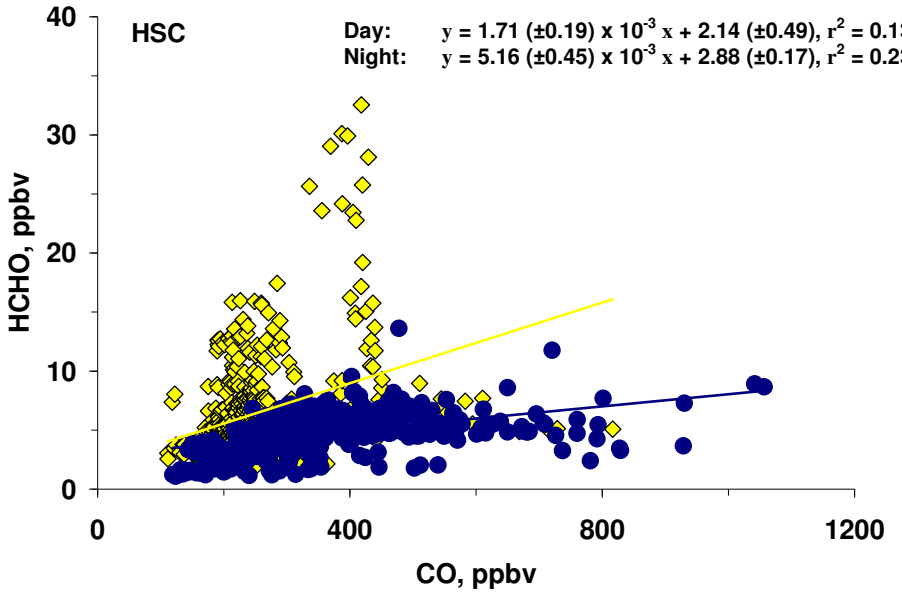

Fig. 6b. Relationships of HCHO to CO obtained at the MT. Designation "HSC" is defined the same way as for Fig. 1. Yellow diamonds represent daytime measurements, blue dots represent nighttime measurements. Night- and daytimes defined as in Fig. 4.

ACPD
9, 24193–24223, 2009

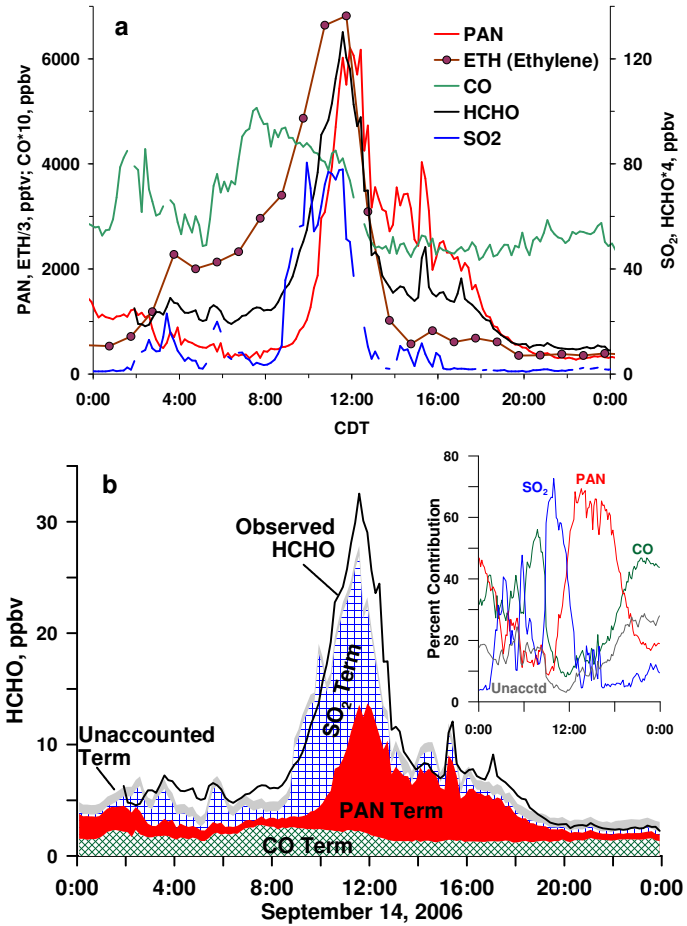

Fig. 7. Case Study. 14 September 2006.

ACPD
9, 24193–24223, 2009

Formaldehyde and its relation to CO, PAN, and SO_2

B. Rappenglück et al.

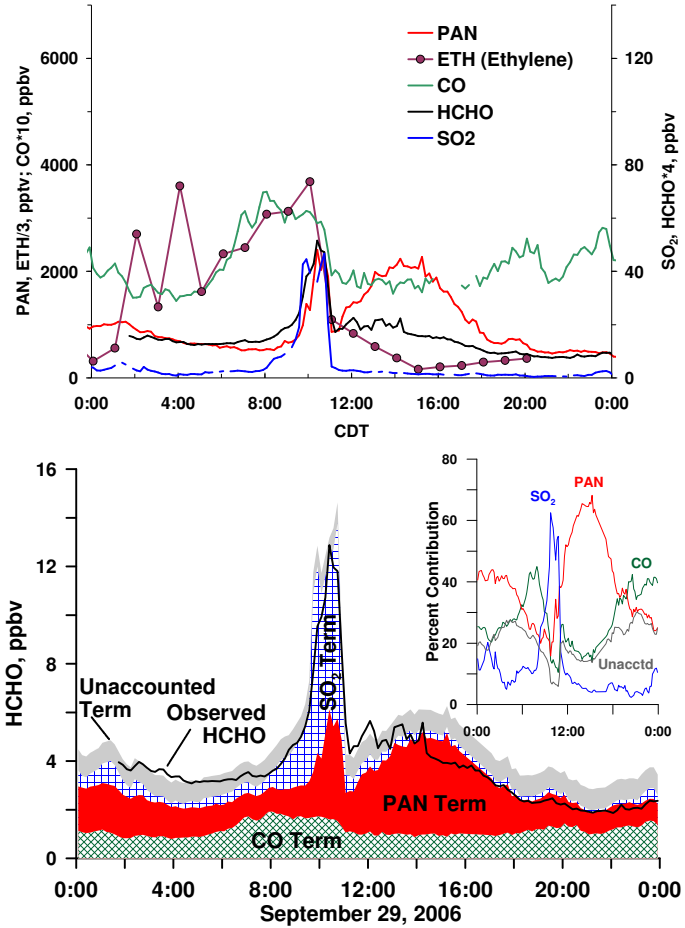

Fig. 8. Case Study. 29 September 2006.

ACPD
9, 24193–24223, 2009

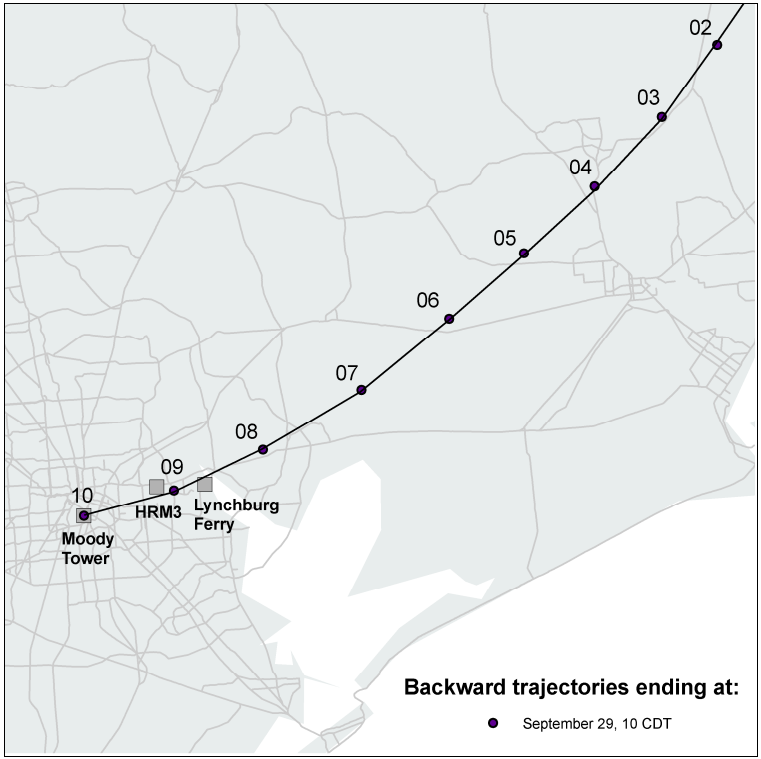

Fig. 9. Backward trajectory analysis for the event of 29 September 2006.

ACPD
9, 24193–24223, 2009

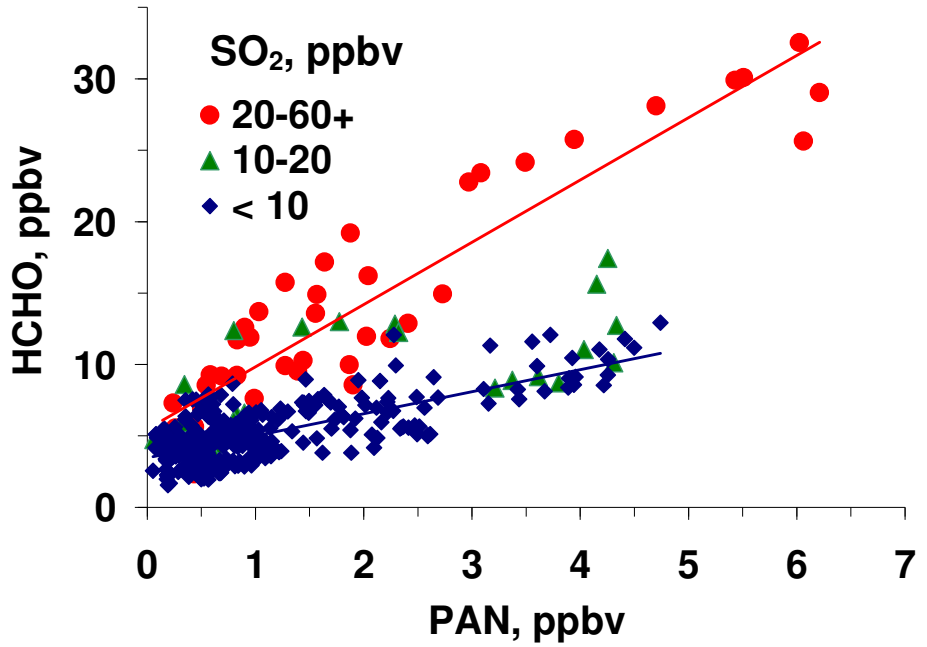

Fig. 10. HCHO-PAN relationships and the role of SO_2.

ACPD
9, 24193–24223, 2009

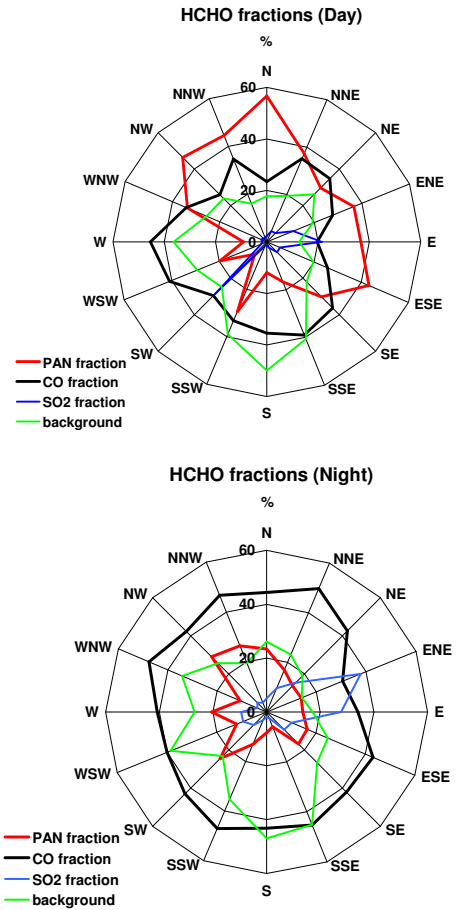

Fig. 11. Median HCHO fractions and their dependencies on wind direction at the MT site. Night- and daytimes defined as in Fig. 4.

ACPD

9, 24193–24223, 2009

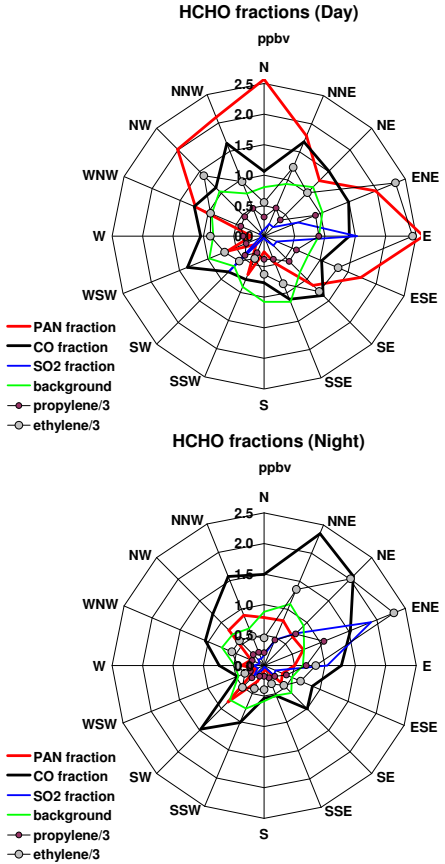

Fig. 12. Contributions to median ambient HCHO mixing ratios based on surrogate species CO, SO_2, and PAN at the MT site. In addition calculated background median HCHO values and observed median mixing ratios of propylene and ethylene are shown. Night- and daytimes defined as in Fig. 4.

ACPD
9, 24193–24223, 2009